

Contact Electrification Using Force Microscopy

B. D. Terris, J. E. Stern,^(a) D. Rugar, and H. J. Mamin

IBM Research Division, Almaden Research Center, 650 Harry Road, San Jose, California 95120-6099

(Received 10 July 1989)

One of the oldest unresolved problems in physics is the mechanism of charge exchange between contacting surfaces when at least one of them is insulating. We describe a new technique, using force microscopy, for studying this problem with greater lateral resolution than has been previously possible. The force microscope is shown to have 0.2- μm lateral resolution and the sensitivity to detect 3 electronic charges. In contact-charging experiments between the microscope tip and polymethyl methacrylate, the charged region was much larger than the expected contact area and bipolar charge exchange was observed.

PACS numbers: 73.40.Bf, 61.16.Di, 73.25.+i, 73.40.Ns

When two surfaces are brought into contact, they will generally exchange charge and when subsequently separated will be oppositely charged. This type of charge exchange between objects is observed in such diverse areas as ice particles in clouds, shoes on carpets, and toner particles in electrophotographic copiers and printers, and has been implicated in grain elevator explosions.¹ Despite its everyday occurrence, the physical explanation of this basic phenomenon of contact electrification, or triboelectrification, has eluded researchers since the times of the ancient Greeks.²

Traditionally, triboelectrification has been classified into three categories: metal-metal, metal-insulator, and insulator-insulator contact. In the first case, when two metals are contacted, Harper³ has demonstrated that electrons flow until the two Fermi levels equilibrate. The process in the later two cases, however, is not well understood and there are contradictory data in the literature. Lowell, Rose-Innes, and El-Kazzaz,⁴ for example, have claimed that on contacting a polymer with a series of metals the net insulator charge depends only on the last metal contacted. In similar experiments, Fabish and Duke⁵ found that the charge on the polymer accumulates with each contacting metal and that each metal acts independently. Based on their observations they proposed a theory of contact-charge spectroscopy wherein each metal accesses different electronic states in the polymer.

At the center of this dispute is the nature of the charge sites. If it were possible to identify such sites with near atomic resolution, then a deeper understanding of the triboelectrification process might result. Most current experiments, however, measure the charge exchanged averaged over millimeter-sized areas. In this Letter we describe a novel approach to studying this problem, where, by using a force microscope, the spatial distribution of charge from a single contact can be imaged with higher resolution than has been possible with other techniques. With further refinement, the technique holds promise for being able to image single charges and to locate the charge sites.

The principles of force microscopy⁶⁻⁸ and the imaging of electrostatic charge with a force microscope have been described in detail elsewhere.⁹⁻¹¹ Briefly, a lever-tip is mounted on a piezoelectric bimorph and oscillated at a frequency ω_1 just above the resonant frequency of the lever. The lever motion is detected by an optical-fiber-based interferometer¹² and a lock-in amplifier. The levers-tips are electrochemically etched Ni wires, with base diameters $\sim 10 \mu\text{m}$ and lengths $\sim 700 \mu\text{m}$. The last 50-100 μm of the wire is bent at a 90° angle to form a tip. Typical spring constants are on the order of 0.2 N/m and resonant frequencies around 25 kHz. As the tip scans the surface, changes in the tip-to-surface force gradient will alter the effective spring constant of the lever, thereby changing its resonant frequency and its amplitude of oscillation. Figure 1 shows a block diagram of the apparatus. A feedback loop adjusts the tip-to-sample spacing so as to maintain a constant oscillation amplitude (constant force gradient). By monitoring the feedback voltage, labeled "z drive" in Fig. 1, contours of constant force gradient are measured.

Localized charge has been imaged previously using force microscopy.^{9,11} The force-gradient contour was peaked over the charged spot, due to the Coulomb at-

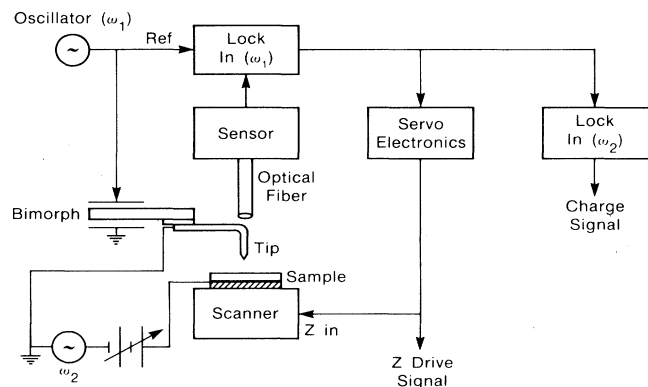


FIG. 1. Block diagram of the force microscope.

traction of the charge to its image charge in the tip. In addition, the image charge in the tip could be altered by applying a voltage to an electrode on the back of the sample. By taking images at several negative and positive electrode biases, the sign of the charge could be determined and charge distinguished from topography.

We have now developed a new mode of imaging which responds only to charge and can distinguish the sign of the charge in a single scan. An ac bias voltage, $V_0 \sin(\omega_2 t)$, is applied between the tip and the electrode behind the dielectric sample, with ω_2 higher than the feedback-loop frequency response, but much lower than ω_1 . This ac voltage induces an oscillating charge on the electrode, $Q_e = CV_0 \sin(\omega_2 t)$, where C is the tip-to-electrode capacitance. An equal and opposite charge is induced on the tip. If there is local static charge, Q_s , on the sample surface, it will also induce an equal and opposite image charge on the tip, and thus the total tip charge is $Q_t = -(Q_s + Q_e)$. To calculate the force on the tip, we treat the tip-surface force as due to point charges and the tip-electrode force as from a capacitor. The electrostatic force on the tip can then be approximated by

$$F_z \approx \frac{Q_s Q_t}{4\pi\epsilon_0 z^2} + \frac{V_0^2 \sin^2(\omega_2 t)}{2} \frac{\partial C}{\partial z},$$

where z is the tip-to-surface spacing. After substituting the expression for Q_t from above, we obtain the force gradient, $F' \equiv \partial F_z / \partial z$, as

$$F' = \frac{V_0^2 \sin^2(\omega_2 t)}{2} \frac{\partial^2 C}{\partial z^2} + \frac{Q_s V_0 \sin(\omega_2 t)}{2\pi\epsilon_0 z^2} \left[\frac{C}{z} - \frac{1}{2} \frac{\partial C}{\partial z} \right] + \frac{Q_s^2}{2\pi\epsilon_0 z^3}.$$

If the surface is uncharged, $Q_s = 0$, only the $\sin^2(\omega_2 t)$ term is nonzero and the force gradient will oscillate at $2\omega_2$. This $2\omega_2$ oscillation in the force gradient will cause the envelope of the ω_1 tip oscillation to be modulated at $2\omega_2$. For charged surfaces, $Q_s \neq 0$, the force gradient has

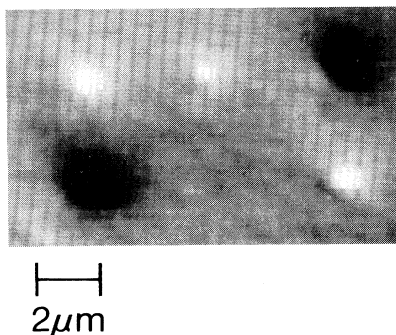


FIG. 2. The charge image of 5 deposited charge regions, 3 positive (white), and 2 negative (black), on a polycarbonate surface.

a $\sin(\omega_2 t)$ term and thus the envelope of the ω_1 tip oscillation will be modulated at ω_2 .¹¹

As shown in Fig. 1, this ω_2 signal is detected at the output of the feedback-loop lock-in amplifier with a second lock-in, and is referred to as the "charge signal." The phase of the detected signal will indicate the sign of the charge. To verify this, we have imaged micron-sized regions of positive and negative charge that were intentionally deposited on a polycarbonate surface. By applying a voltage to the tip and contacting it to the surface, charge of either polarity could be deposited, with the sign of the charge determined by the polarity of the applied voltage.^{9,11} One such charge pattern, with 3 positive (white) and 2 negative (black) charge regions, is shown in Fig. 2.

The charge-imaging technique has been utilized in a novel approach to studying metal-insulator contact electrification. The surface was tribocharged by slowly approaching it to the tip and then allowing the van der Waals attraction to pull the tip into the surface. No voltage was applied to the tip in these contact-charging experiments. The tip was then retracted and used to image the resulting charge deposit. The contact time was on the order of a few seconds and the surface was a 1-mm-thick coupon of polymethyl methacrylate (PMMA). All of the experiments were performed in air at ambient laboratory conditions. The PMMA was of optical-disk quality¹³ and a protective plastic coating was removed from its surface just prior to mounting it on the force microscope. An 8-V p-p. ac voltage was used in the ac bias imaging.

After touching the tip to the surface, a 10- μ m-diam charged region is seen in the charge image (Fig. 3). Note that this area contains both positive (white) and negative (black) charge regions and is substantially larger than the expected contact area. Both the charged area and the details of the charge distribution varied from sample to sample, with some samples having only

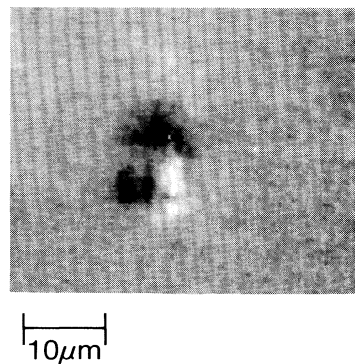


FIG. 3. The charge image of the PMMA surface after it had been contacted by the Ni tip. The black regions are negatively charged and the white regions positively charged.

one sign of charge. Since our experiments were performed in air, there is likely to be adsorbed water on the PMMA surface, which may contribute to the sample-to-sample variations of the charge images. The predominant sign of charge observed was positive, which agrees with electrostatic voltmeter measurements on the same PMMA after it had been contacted by a piece of the Ni wire from which the tip was etched. After some of the tip contacts, the charge pattern was seen to change in time, with the positive and negative regions changing at different rates. After several days, most charge spots had decayed away.

We can only speculate on the source of the bipolar charge patterns. The bipolar transfer of charge would be possible if there were both donor and acceptor states on the surface. This does not, however, explain the spatial extent of the charge. If the surface conductivity is high enough to permit charge spreading, then one might expect the charge to recombine. This would then make the observation of bipolar charge difficult to understand. An alternative explanation is that there may be an electrical breakdown near the tip as it is separated from the surface. This will tend to discharge the surface, but may also overcompensate so that areas of both charge polarities remain.¹⁴ This breakdown would be sensitive to the initial charge density, rate of tip withdrawal, and exact tip shape.

This bipolar charging is a surprising result and, to our knowledge, has not been observed in previous tribocharging experiments. Because of their limited lateral resolution, previous measurements, which typically use electrostatic voltmeter techniques, would only have seen the net charge in a much larger, millimeter-sized, region. By contacting a metal sphere to numerous spots of a polymer surface, Lowell and Akande¹⁵ have studied the spot-to-spot variation in the polymer charge. They found a broad, and often bipolar, distribution of charging levels. If our results are general and the charge exchanged

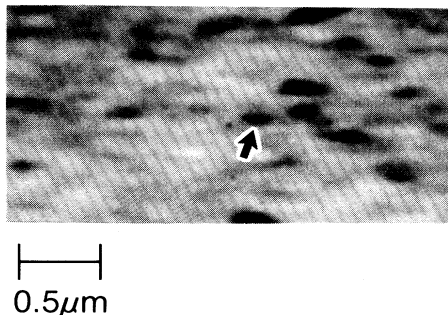


FIG. 4. The charge image for an oxidized Si surface after it had been bombarded by 0.3- μm polystyrene spheres. The smallest, well defined, negatively charged (black) regions are approximately 0.2 μm in diameter. One such region is marked by the arrow.

is bipolar in each contact to a small area, then the net charge will be a delicate balance of these regions, and one might expect to measure broad distributions of charging levels.

The charge regions in Fig. 3 are much larger than the instrument's lateral resolution for charge imaging. To demonstrate the charge-imaging resolution, it is necessary to produce smaller charge regions. One method to locally charge a surface is to bombard it with small insulating particles. Shown in Fig. 4 is the charge image of a Si surface (with its native oxide) after it had been bombarded by 0.3- μm polystyrene spheres. Charge features as small as 0.2 μm can be seen in the image. The corresponding feedback-voltage image showed little structure, indicating that the spheres did not adhere to the surface and that the charge level was below the detection limit of the feedback-imaging mode. The origin of these charge regions is likely tribocharging between the oxidized Si surface and the polystyrene spheres.

In addition to this excellent lateral resolution, which is unsurpassed by other charge-imaging techniques, the force microscope also has very high sensitivity to charge. Using the feedback-imaging mode, we had previously estimated a detection limit of 100 electronic charges at a scanning height of 500 \AA .⁹ We have now found that this new imaging mode has an order of magnitude greater sensitivity. This sensitivity can be estimated by applying a dc bias voltage between a conducting substrate and the microscope tip. The minimum detectable dc voltage, found to be 0.02 V, can then be converted to an equivalent charge from the tip-to-sample capacitance.

To calculate the capacitance, we model the system as a sphere of radius R above a metal plane with capacitance¹⁶

$$C = 4\pi\epsilon_0 R \sinh\alpha \sum_{n=1}^{\infty} (\sinh n\alpha)^{-1},$$

where $\alpha = \cosh^{-1}(H/R)$ and $H = R + z$ is the distance from the surface to the center of the charge sphere. The two parameters, tip radius R and height z , were found by fitting the force gradient corresponding to this capacitance to the measured force gradient. The measured force gradient as a function of z is shown in Fig. 5 for two values of the applied dc bias voltage. The force gradient was determined from the frequency shift δf according to $F' = 2k\delta f/f_0$, where f_0 is the tip resonant frequency.⁷ The lever spring constant k was calculated from the lever geometry to be 0.2 N/m. The best fit to the data, shown by the solid curve in Fig. 5, was obtained with a tip radius of $1500 \pm 500 \text{\AA}$, in good agreement with estimates from scanning-electron-microscope measurements, and by adding $900 \pm 300 \text{\AA}$ to the measured tip-to-sample spacing.¹⁷ Using these fitting parameters, and a typical tip-to-sample spacing of 500 \AA , we calculate a tip-to-sample capacitance of $2.26 \times 10^{-17} \text{ F}$. The minimum detectable dc voltage of 0.02 V then corre-

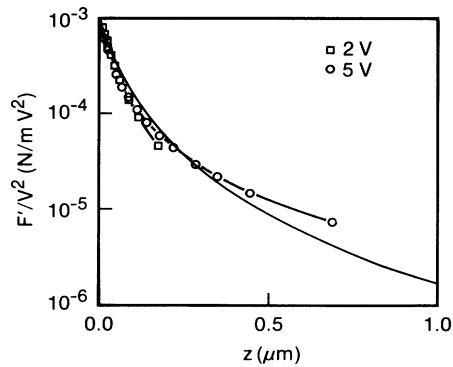


FIG. 5. The force gradient, normalized to the square of the dc bias, as a function of tip-to-sample spacing. The open symbols show the data for two values of the dc bias. The lines connecting the points are guides to the eye. The solid line is the force gradient calculated from a sphere-to-plane capacitance model and fitted to the data. As expected for a capacitor, the force gradient varies as the voltage squared.

sponds to an equivalent charge of 3 ± 1.5 electrons. Even greater sensitivity should be achievable by scanning closer to the sample.

The authors gratefully acknowledge helpful discussions with J. C. Scott, G. Hadziioannou, G. McClelland, R. F. Hoyt, and T. C. Reiley. We thank B. Hahn for providing the samples and F. Saurenbach for taking the data in Fig. 2.

^(a)Present address: IBM General Technology Division, 1000 River Street, Essex Junction, Vermont 05452.

¹J. A. Cross, *Electrostatics, Principles, Problems and Applications* (Adam Hilger, Bristol, 1987).

²For a general review, see J. Lowell and A. C. Rose-Innes, *Adv. Phys.* **20**, 947 (1980); L. B. Schein, *Electrophotography*

and *Development Physics* (Springer-Verlag, Berlin, 1988), Chap. 4.

³W. R. Harper, *Contact and Frictional Electrification* (Clarendon, Oxford, 1967).

⁴J. Lowell, A. C. Rose-Innes, and A. M. El-Kazzaz, *J. Appl. Phys.* **64**, 1957 (1988), and references therein.

⁵T. J. Fabish and C. B. Duke, *J. Appl. Phys.* **64**, 2218 (1988), and references therein.

⁶G. Binnig, C. F. Quate, and Ch. Gerber, *Phys. Rev. Lett.* **56**, 930 (1986).

⁷Y. Martin, C. C. Williams, and H. K. Wickramasinghe, *J. Appl. Phys.* **61**, 4723 (1987).

⁸G. M. McClelland, R. Erlandsson, and S. Chiang, in *Review of Progress in Quantitative Nondestructive Evaluation*, edited by D. O. Thompson and D. E. Chimenti (Plenum, New York, 1987), Vol. 6B, p. 307.

⁹J. E. Stern, B. D. Terris, H. J. Mamin, and D. Rugar, *Appl. Phys. Lett.* **53**, 2717 (1988).

¹⁰Y. Martin, D. W. Abraham, and H. K. Wickramasinghe, *Appl. Phys. Lett.* **52**, 1103 (1987).

¹¹B. D. Terris, J. E. Stern, D. Rugar, and H. J. Mamin, *J. Vac. Sci. Technol.* (to be published).

¹²D. Rugar, H. J. Mamin, R. Erlandsson, J. E. Stern, and B. D. Terris, *Rev. Sci. Instrum.* **59**, 2337 (1988).

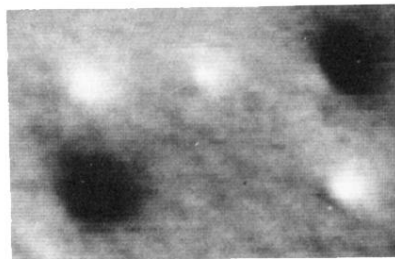
¹³PMMA obtained from Rohm GmbH, Darmstadt, Germany.

¹⁴X. G. Ji, Y. Takahashi, Y. Komai, and S. Kobayashi, *J. Electrostat.* **23**, 381 (1989).

¹⁵J. Lowell and A. R. Akande, *J. Phys. D* **21**, 125 (1988).

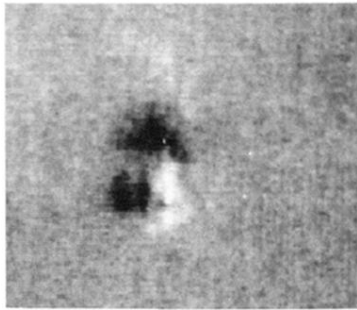
¹⁶E. Durand, *Electrostatique* (Masson, Paris, 1966), Vol. II, p. 209.

¹⁷The additional tip-to-sample spacing may arise from at least two sources. The first is a reflection of the fact that the tip is shaped more like a paraboloid than a sphere. Therefore, due to the tip's elongated nature, the charge centroid would be shifted away from the sample surface. Second, the tip position relative to the sample surface is determined by moving the sample until the tip contacts the surface and the oscillation (at ω_1) amplitude goes to zero. Any static deflection of the lever is therefore unaccounted for and would result in an underestimate of the true distance.



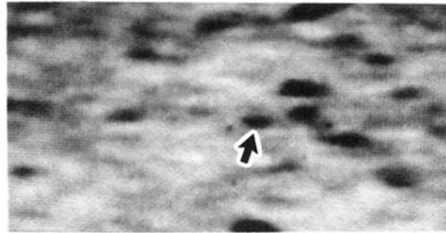
—|—
2 μ m

FIG. 2. The charge image of 5 deposited charge regions, 3 positive (white), and 2 negative (black), on a polycarbonate surface.



10 μ m

FIG. 3. The charge image of the PMMA surface after it had been contacted by the Ni tip. The black regions are negatively charged and the white regions positively charged.





0.5 μm

FIG. 4. The charge image for an oxidized Si surface after it had been bombarded by 0.3- μm polystyrene spheres. The smallest, well defined, negatively charged (black) regions are approximately 0.2 μm in diameter. One such region is marked by the arrow.